Macromolecules

pubs.acs.org/Macromolecules Article

Distinct Viscoelasticity of Hierarchical Nanostructures Self-Assembled from Multiblock Copolymers

Wei Hong, Jiaping Lin,* Xiaohui Tian, and Liquan Wang*

Cite This: *Macromolecules* 2020, 53, 10955−10963 Read Online

ACCESS | Metrics & More | Article Recommendations | Supporting Information

ABSTRACT: We employed a nonequilibrium dissipative particle dynamics method to study viscoelastic properties of hierarchical lamellar structures self-assembled from heptablock copolymers. Three ways of shearing with respect to lamellar planes, including parallel, vertical, and transverse shearing, were imposed to study the viscoelasticity of ordered systems. In parallel shear, with the morphology transformation from disorder to general lamellae to parallel lamellae-in-lamella, both the storage and loss moduli of multiblock copolymer melt show a remarkable improvement. In addition to the parallel lamellae-in-lamella, the multiblock copolymers can form perpendicular lamellae-in-lamella with different viscoelastic behaviors. In vertical shear, parallel lamellae-in-lamella shows terminal behavior, while a low-frequency plateau in the storage modulus exists for the perpendicular lamellae-in-lamella. In transverse shear, the storage moduli for both perpendicular and parallel lamellae-in-lamellae with strong separation of small-length-scale structure exhibit a solid-like plateau at low frequency. The physical origin underlying the distinct viscoelasticity of various hierarchical lamellae was revealed by monitoring the motions of polymer blocks at different length scales. The present work could provide information for preparing advanced materials based on packed lamellae.

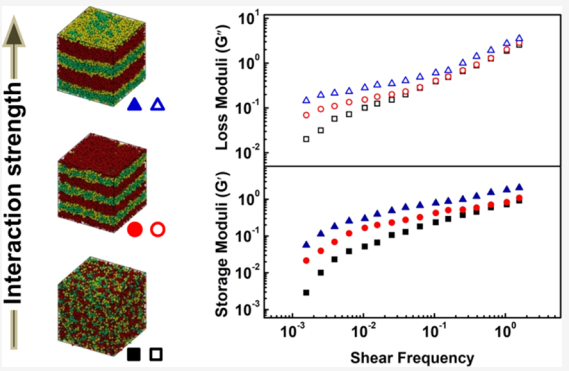

1. INTRODUCTION

Microphase-separated structures, combining physical and chemical properties of various components in a material, lay the foundation of block copolymer applications.[1] Different domains in the phase-separated structures offer distinctly different properties. For instance, in diblock copolymers containing rubbery and glassy domains, the rubbery spheres can improve the impact resistance of the glassy matrix, while the glassy spheres can enhance the mechanical strength of the rubbery matrix.[2,3] The integration of different properties offered by different domains relies on the geometry of phase-separated structures. As such, various kinds of block copolymers have been developed to expand the portfolio of ordered phases.[4−6] Multiblock copolymers are appealing for their dramatically enhanced mechanical properties such as impressive toughness and easy processability because the accessible order−disorder transition temperature can be decoupled from the total molecular weight of polymers.[2]

Multiblock copolymers are capable of phase-separating into hierarchical structures with two or more different periodicities. Matsushita *et al.* prepared a linear $P(IS)_4IP$ undecablock terpolymer, where the poly(2-vinylpyridine) (P) is strongly incompatible with the polyisoprene (I) and the polystyrene (S).[7] They found that the copolymers can phase separate into hierarchical lamellar structures with two crystallographic periods. Apart from the parallel packed lamellar structures, more complex morphologies such as spheres-in-lamellae and cylinders-in-lamellae were observed.[8] Bates and Fleury synthesized nearly monodisperse CEC-P tetrablock copolymers and $(CEC)_2$-P heptablock copolymers, which consists of identical volume fractions of poly(ethylene-*alt*-propylene) (P) and compositionally symmetric CEC (here C and E are poly(cyclohexylethylene) and polyethylene, respectively).[9,10] They identified perpendicular lamellae between two parallel lamellae in these samples. A central theme of the design of multiblock copolymers is to improve the mechanical properties by combining different properties offered by different components. Bates and Fleury found that microphase separation of tetrablock/heptablock copolymers into hierarchical lamellar structures results in mechanically resilient materials.[10] The vitrification and crystallization of different blocks can significantly influence the mechanical properties of polymers. In general, the experimental samples are isotropic, which contains many oriented domains with grain boundaries. As such, it is difficult to reveal the contribution of domain orientations to the viscoelasticity of hierarchical structures.

Received: September 11, 2020
Revised: November 18, 2020
Published: December 2, 2020

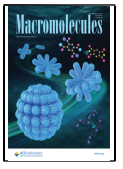

Downloaded via EAST CHINA UNIV SCIENCE & TECHLGY on December 24, 2020 at 05:23:24 (UTC).
See https://pubs.acs.org/sharingguidelines for options on how to legitimately share published articles.

ACS Publications © 2020 American Chemical Society

https://dx.doi.org/10.1021/acs.macromol.0c02096
Macromolecules 2020, 53, 10955−10963

Theory and simulation can help understand the effect of domain orientation on the viscoelasticity by obtaining ordered hierarchical structures.

Theory and simulation are of particular use to develop a fundamental understanding of the structure−property relationship of the hierarchical structures.[11−14] On the aspect of structure studies, self-consistent field (SCFT) theory and dissipative particle dynamics (DPD) simulation have successfully been used to predict the structures and morphologies constituted by the multiblock copolymers.[15−20] Lin and coauthors have used SCFT and DPD to reproduce a series of hierarchical structures found in the experiments.[21,22] On the aspect of property studies, nonequilibrium molecular dynamics (NEMD) simulations are widely utilized to examine the rheological properties of block copolymers.[23−25] Ganesan *et al.* combined nonequilibrium oscillatory shear technique and DPD simulation to study the viscoelastic properties of ABA triblock copolymers, which can form a gel in solution due to the amphiphilic interactions.[26] They demonstrated that their simulation results show a high coincidence with other theoretical calculations and experimental findings. Xu *et al.* also utilized the NEMD simulation to study the viscoelastic properties of nanoparticle-tethering polymers.[27] It was found that tethering nanoparticles with polymer chains can enhance the storage and loss moduli compared to bare blends of nanoparticle and polymers.

In an earlier study, we combined the SCFT calculation and linear elastic theory to explore the elastic properties of multiblock copolymers with hierarchical lamellar structures.[28] There, we focused on the tensile moduli and shear moduli of the hierarchical lamellar structures and found that the hierarchical structure design can improve the moduli of the polymers. In the present work, we seek to use the DPD simulation and nonequilibrium oscillatory shear technique to study the rheology of the polymer melts with hierarchical structures. The hierarchical structures are formed by the microphase separation of linear $(\mathbf{ABA})_2$-**C** heptablock copolymers similar to the experimentally reported $(\mathrm{CEC})_2$-P heptablock copolymers.[2,29] General lamellae and two kinds of hierarchical lamellar structures, including parallel and perpendicular lamellae-in-lamellae, were acquired, and their viscoelastic responses were examined. It was found that the viscoelasticity is closely associated with the shear direction and packing of lamellar structures. Especially in parallel shear with respect to the lamellar plane, the viscoelasticity of heptablock copolymers is enhanced significantly with the formation of hierarchical structures. We expect that the present work could provide a comprehensive understanding of the relationships between the structure and viscoelasticity of multiblock copolymers.

2. METHODS AND MODEL

2.1. Dissipative Particle Dynamics. We used DPD methods to study the self-assembly and rheological behavior of multiblock copolymers. The DPD simulations have been widely adopted to explore the dynamic and rheological properties of complex fluids at the mesoscopic scales.[30,31] In the method, the movement of each DPD bead is governed by the Newtonian equations of motion, $\mathrm{d}\mathbf{r}_i/\mathrm{d}t = \mathbf{v}_i$ and $m\mathrm{d}\mathbf{v}_i/\mathrm{d}t = \mathbf{f}_i$, where m is the mass of each bead, $\mathbf{v}_i$ and $\mathbf{r}_i$ represent the velocity and position of bead i, respectively, and $\mathbf{f}_i$ is the force exerted on it. The force ($\mathbf{f}_i$) contains four parts, that is, a conservation force F_{ij}^{C}, a dissipative force F_{ij}^{D}, a random force F_{ij}^{R}, and a spring bond force F_{ij}^{S}. The adjacent beads in the multiblock copolymer chains are connected *via* the spring bond force $F_{ij}^{\mathrm{S}} = C(1 - r_{ij}/r_{\mathrm{eq}})\hat{r}_{ij}$ with equilibrium bond distance $r_{\mathrm{eq}} = 0.86$ and spring constant $C = 100$. We adopted reduced units for all physical quantities. The units of mass, length, and energy are m, r_{c}, and $k_{\mathrm{B}}T$, respectively, where k_{B} is the Boltzmann constant, and T is the temperature. Based on the above physical quantities, we can obtain the time unit of $\tau = (mr_{\mathrm{c}}^2/k_{\mathrm{B}}T)^{1/2}$.[32] The details of the DPD method can be found in Section 1 of Supporting Information.

2.2. Nonequilibrium Simulation. In order to govern the viscoelastic properties of multiblock copolymers, we adopt a nonequilibrium oscillatory shear technique entailing beads with an additional velocity in the shear direction. The "box deforming" technique adopted in this work is conceptually identical to the Lees-Edward boundary conditions, which were the most widely used to produce a shear field.[26,27,33,34] For $x-y$ plane shear (x- and y-direction are shear direction and velocity gradient, respectively), the motion equation of the bead i with SLLOD algorithm takes form as follow

$$\frac{\mathrm{d}\mathbf{r}_i}{\mathrm{d}t} = \mathbf{v}_i + \mathbf{e}_x\dot{\gamma}r_{i,y} \qquad m_i\frac{\mathrm{d}\mathbf{v}_i}{\mathrm{d}t} = \mathbf{f}_i - m_i\mathbf{e}_x\dot{\gamma}v_{i,y} \tag{1}$$

where $v_{i,y}$ and $r_{i,y}$ are the magnitudes of the velocity and position vector (here, the subscript y represents the y-component of a vector), respectively. $\mathbf{e}_x$ is the normalized vector along the x-direction. The $\dot{\gamma}$, called shear rate, is the time derivative of shear strain γ. The box is subjected to an alternating strain, and the stress is measured simultaneously. Both the strain and stress alter sinusoidally as the equilibrium is achieved, but the strain lags behind the stress. The lag angle, called phase angle, is defined as δ. The mathematical expressions are as follows

$$\gamma = \gamma_0\sin(\omega t), \qquad \sigma_{xy} = \sigma_0\sin(\omega t + \delta) \tag{2}$$

the stress consists of two components, that is, G' sin ωt and G'' cos ωt. Here, G' is the storage modulus and G'' is the loss modulus

$$G' = \frac{\sigma_0}{\gamma_0}\cos(\delta), \qquad G'' = \frac{\sigma_0}{\gamma_0}\sin(\delta) \tag{3}$$

We can obtain σ_{xy} readily through the tensor version of the virial theorem given by

$$\sigma = \frac{1}{V}\left\langle \sum_i m_i\boldsymbol{v}_i\boldsymbol{v}_i + \frac{1}{2}\sum_{i\neq j}\boldsymbol{r}_{ij}\boldsymbol{F}_{ij} \right\rangle \tag{4}$$

Here, V represents the volume of the simulation box, and the angular bracket denotes an ensemble average.

2.3. Model and Condition. In the simulations, we constructed a coarse-grained model of $(\mathbf{A}_3\mathbf{B}_6\mathbf{A}_3)_2$-$\mathbf{C}_{24}$ multiblock copolymer based on the experimentally reported $(\mathrm{CEC})_2$-P heptablock copolymers.[2,29] The subscript in $(\mathbf{A}_3\mathbf{B}_6\mathbf{A}_3)_2$-$\mathbf{C}_{24}$ represents the length of each block, as typically shown in Figure 1a. Different kinds of hierarchical lamellae-in-lamellar structures were obtained by regulating interaction strengths between various blocks. The viscoelastic properties of those structures were investigated by imposing an oscillatory strain. It needs to stress that the interaction strengths have a less marked influence on the characteristic response of ordered structures in the low-frequency region. Due to the anisotropic characteristic of the lamellar structure, there are three orthogonal orientations of the lamellar structure with respect to the imposed shear, as schematically illustrated in Figure 1b. The shear plane, along with the lamellar plane of the lamellar structure, is denoted by parallel shear. The vertical shear represents that the shear plane is perpendicular to the lamellar plane, and the shear direction is along with the orientation of the lamellar plane. The transverse shear means that the shear plane is perpendicular to the lamellar plane, and the shear direction is normal to the orientation of the lamellar plane.

A triclinic (non-orthogonal) cubic box was adopted in the simulations, where periodic boundary conditions and the *NVT* ensemble were applied. The interaction strengths for different types of particles are listed in Table 1. The noise amplitude σ and friction coefficient γ are set to be 3.0 and 4.5, respectively, and thus $k_{\mathrm{B}}T = 1.0$. The box size was selected carefully to make the layer plane parallel to

https://dx.doi.org/10.1021/acs.macromol.0c02096
Macromolecules 2020, 53, 10955−10963

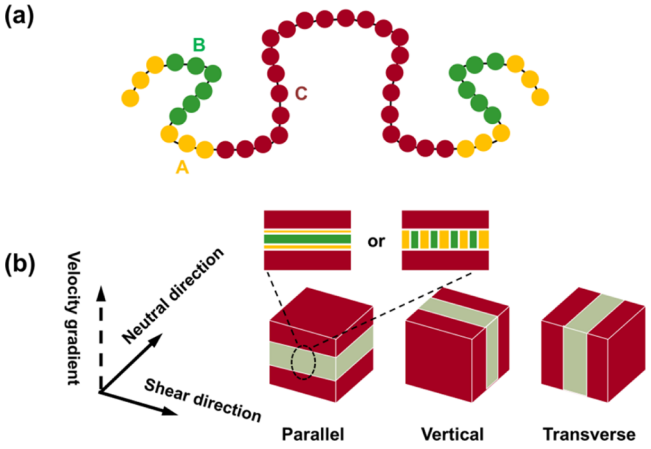

Figure 1. (a) DPD model of $(\mathbf{ABA})_2$-**C** multiblock copolymers. The yellow, green, and red colors are assigned to **A**, **B**, and **C** blocks, respectively. (b) Schematic of orthogonal orientations of the lamellar structure imposed to shear. The tawny layer represents the small-length-scale structure with two possible arrangements.

Table 1. Interaction Parameters a (in DPD Unit) Used in the Simulations

	A	B	C
A	25		
B	25−80	25	
C	25, 50, 120	25, 40, 50	25

the face of the box. A box of $22.6 \times 22.6 \times 22.6\ r_c^3$ was adopted for all systems except the perpendicular lamellae-in-lamella system in which the box size was $20.8 \times 20.8 \times 20.8\ r_c^3$. The velocity-Verlet algorithm was applied to integrate the equations of motion with a time step of $\Delta t = 0.04\tau$. 6×10^6 DPD steps were performed so that there is enough time for these systems to reach equilibrium. After the equilibrium structures were obtained, the nonequilibrium oscillatory shear technique was applied by oscillating the tilt factor sinusoidally with the specified amplitude and period. The software, large atomic/molecular massively parallel simulator, was used in the simulations.[35]

3. RESULTS AND DISCUSSION

The work presents a study on the viscoelastic properties of hierarchical lamellae-in-lamellar structures with various orientations. The hierarchical lamellar structures are formed by the self-assembly of the heptablock copolymers sketched in Figure 1a (note that the beads of **A**, **B**, and **C** block were assigned with yellow, green, and red colors, respectively). Before viscoelasticity studies, we applied the DPD simulation to gain various lamellae-in-lamellar structures by choosing various kinds of interaction strengths.

The representative lamellar structures are presented in Figure 2. Disordered phase (**D**) was obtained at lower interaction strengths ($a_{AB} = a_{AC} = a_{BC} = 25$, Figure 2a). Increasing the repulsive interaction between the **A** (and **B**) block and **C** block leads to the formation of general lamellar structure (**L1**, $a_{AB} = 25$, $a_{AC} = a_{BC} = 50$, Figure 2b). As the repulsive interaction between **A** and **B** blocks further increases, the **A** and **B** phases are gradually separated and a structural transformation from lamellae to lamellae-in-lamella was observed (**L2**, $a_{AB} = 30$, $a_{AC} = a_{BC} = 50$, Figure 2c; **L3**, $a_{AB} = 35$, $a_{AC} = a_{BC} = 50$, Figure 2d; $\mathbf{L_2}\mathbf{1}$, $a_{AB} = 40$, $a_{AC} = a_{BC} = 50$, Figure 2e). The parallel lamellae-in-lamellar structure with well-segregated **A** and **B** domains are formed with a larger repulsive interaction ($\mathbf{L_2}\mathbf{2}$, $a_{AB} = 80$, $a_{AC} = a_{BC} = 50$, Figure 2f).

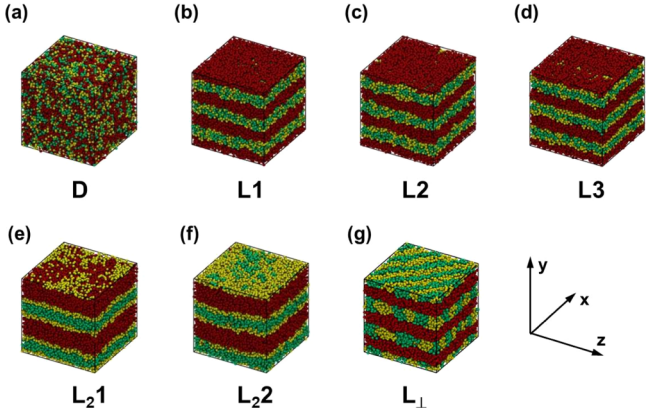

Figure 2. Snapshots of hierarchical structures self-assembled from $(\mathbf{ABA})_2$-**C** multiblock copolymers with various interaction strengths in the bulk: (a) **D**, $a_{AB} = a_{AC} = a_{BC} = 25$, (b) **L1**, $a_{AB} = 25$, $a_{AC} = a_{BC} = 50$, (c) **L2**, $a_{AB} = 30$, $a_{AC} = a_{BC} = 50$, (d) **L3**, $a_{AB} = 35$, $a_{AC} = a_{BC} = 50$, (e) $\mathbf{L_2}\mathbf{1}$, $a_{AB} = 40$, $a_{AC} = a_{BC} = 50$, (f) $\mathbf{L_2}\mathbf{2}$, $a_{AB} = 80$, $a_{AC} = a_{BC} = 50$, and (g) $\mathbf{L}_\perp$, $a_{AB} = 60$, $a_{AC} = 120$, $a_{BC} = 40$.

For comparison, we also generated a perpendicular lamellae-in-lamellar structure ($\mathbf{L}_\perp$) by setting the interaction parameters according to our previous work ($a_{AB} = 60$, $a_{AC} = 120$, $a_{BC} = 40$, Figure 2g).[22] Notably, in the expressions such as $\mathbf{L_2}\mathbf{1}$, the first bold letter, subscript, and last number represents lamellae, parallel lamellae-in-lamella (the symbol $\perp$ represents perpendicular lamellae-in-lamella in which the small-length-scale lamellae are perpendicular to the large-length-scale lamellae), and the sample number. These hierarchical structures are consistent with those reported in the experiments.[7,10] We also plotted the density profiles of the structures, which is shown in Figures S1 and S2. The density profiles can clearly show the phase separation of **A** and **B** blocks in small-length-scale lamellae. The well-segregated small-length-scale structures were observed in $\mathbf{L_2}\mathbf{1}$, $\mathbf{L_2}\mathbf{2}$, and $\mathbf{L}_\perp$ systems. After acquiring the equilibrium structures, we conducted nonequilibrium DPD simulations to explore the viscoelastic properties of the hierarchical lamellar structures under oscillatory shear.

3.1. Linear Viscoelasticity of Parallel Lamellar Structures. This section presents the results for the linear viscoelasticity of the parallel hierarchical structures obtained by imposing an oscillatory shear. It is well known that the rheology of microphase-separated block copolymers is highly sensitive to strain amplitude.[36] The value of strain amplitude was first considered to guarantee that the systems are in the linear viscoelastic region.

Figure 3 shows the dependence of storage (G') and loss (G'') moduli on the strain amplitude for the representative systems given in Figure 2 under parallel shear with frequency of $\omega = 0.0628\tau^{-1}$. For all systems, the dependency shows two distinct regions, that is, strain independence in the small-strain region and strain dependence in the large-strain region. Similar phenomena can also be observed in vertical/transverse shear. The equilibrium structures are not destroyed in the small-strain region, leading to the plateaus of G' and G''. With the increase of strain amplitude, G' gradually decreases (strain softening) while G'' displays a noticeable maximum value (strain hardening), which stems from the structural failure and the rise of energy dissipation. In addition, the G' (and G'') increases as the structure of systems changes from a disordered state to general lamellae and then to hierarchical lamellae-in-lamella. Notably, the parallel lamellae-in-lamellar structure

https://dx.doi.org/10.1021/acs.macromol.0c02096
Macromolecules 2020, 53, 10955−10963

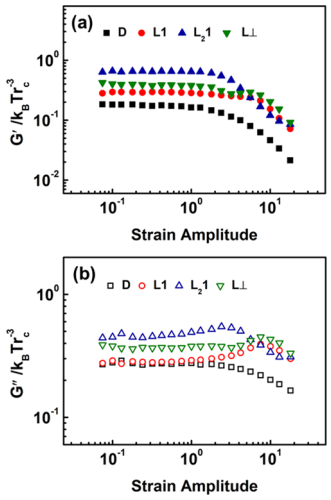

Figure 3. Plots of (a) storage (G') and (b) loss moduli (G'') as a function of strain amplitude for various structures under parallel shear with the frequency of $\omega = 0.0628\tau^{-1}$.

shows a larger storage and loss moduli relative to the perpendicular lamellae-in-lamellar structure. According to the above results, the strain γ was maintained at a value of 0.1 in the following simulation, which is in the linear region of the viscoelastic response.

3.2. Dependence of Moduli on Shear Frequency. We then studied the linear viscoelasticity of parallel lamellae at three different shear directions to examine the dependence of moduli on the shear frequency. The results are as shown in Figure 4. The data at lower frequencies are not presented due to the sharp thermal fluctuation. Kossuth *et al.* found that the storage and loss moduli of block polymer are sensitive to the state of ordering at low frequencies: the disordered liquid state shows a terminal behavior of $G' \sim \omega^2$ and $G'' \sim \omega$,[1] while the ordered state shows distinct viscoelasticity in which both the power-law exponents of G' and G'' are less than one.[36] The G' and G'' of disordered phases (**D**) obtained by imposing a shear in all three directions are close to each other due to the isotropic characteristic. Therefore, we used the average of all data acquired from the three directions to get smooth estimates of the modulus. As shown in Figure 4, the G'' is larger than the G' in **D** system over the whole frequency range, indicating liquid-like viscoelasticity. The $G' \sim G'' \sim \omega^{0.5}$ in the high-frequency region, and terminal behavior of $G' \sim \omega^2$ and $G'' \sim \omega^1$ in the low-frequency region were observed in the disordered state, which generally follows the Rouse dynamics.[37,38] It should note that the position of the turning point in the G' is related to the slowest relaxation time of the polymers. By calculating the normal modes for each polymer chain, we can obtain the Rouse relaxation time (the slowest relaxation time) of polymer chains in the disordered system.[39] The Rouse relaxation time has a value of 268.0τ, as shown in Figure S3, providing reasonable estimates of the frequency at which the storage moduli displays a turning point ($\omega = 1/t = 0.00373\tau^{-1}$).

Figure 4a shows the curves of G' and G'' as a function of shear frequency obtained by parallel shearing. For clarity, the G' and G'' of ordered structures are shifted vertically, and the shift factors k are equal to 1,10,10^2,10^3,10^4, and 10^5 for **D**, **L1**, **L2**, **L3**, $\mathbf{L_21}$, and $\mathbf{L_22}$ systems, respectively. With the structure evolution from disordered (**D**) to ordered (**L1**) phase, two distinct crossovers are evident in G' and G'' plot. The crossover points at lower and higher frequencies are denoted as ω_c and ω_d, respectively. We can see that as the interaction strength between **A** and **B** blocks increases gradually (the structures change from general lamellae to hierarchical lamellae), the ω_c remains almost constant near $0.01\tau^{-1}$ (close to the longest relaxation time in the **D** system), while the ω_d shifts to a larger frequency. The transition at ω_c could be attributed to the relaxation of the **C** block, that is, the large-length-scale structure. On the other hand, the relaxation of small-length-scale structure, that is, the **A** and **B** block, could result in the crossover at higher frequency ω_d. As the interaction parameter between A and B increases, the strong phase separation of **A** and **B** emerges, leading to a shift of ω_d to a larger frequency. In addition, the terminal behavior of $G' \sim \omega^2$ and $G'' \sim \omega^1$ at frequencies below ω_c was also observed for general and hierarchical lamellae.

Figure 4b shows the dynamic moduli calculated by vertical shearing. It can be seen that general and hierarchical lamellae exhibit liquid-like viscoelasticity ($G' < G''$) over the entire frequency region. Both the variation and value of the dynamic moduli of the lamellar structure are similar to the disordered phase. The reason is that the polymer beads can move along the lamellar plane to relax the stress. This can be understood by examining the dynamics of polymer chains by calculating their mean square displacements (MSDs). The MSDs of **C**

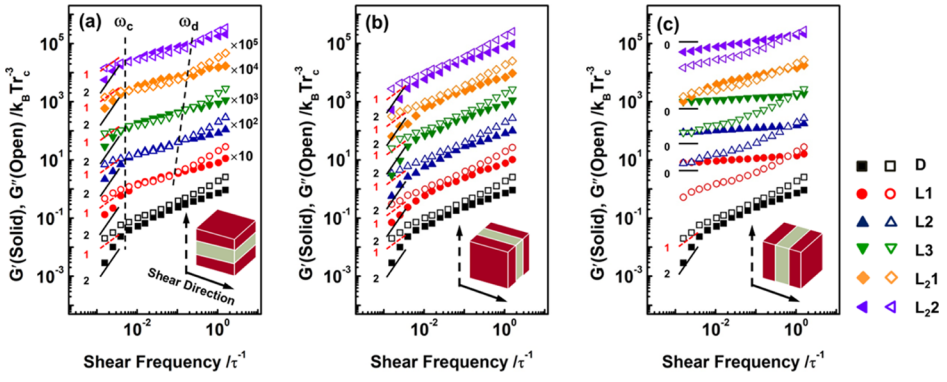

Figure 4. Vertically modulus-shifted master curves for the storage (G') and loss moduli (G'') as a function of shear frequency for various structures with various directions of shear: (a) parallel, (b) vertical, and (c) transverse. In (b) and (c), the shift factors appear as same as those in (a). Insets at the bottom of (a), (b), and (c) are schematic illustrations of three shearing ways, where the solid arrow represents shear direction, and the dashed arrow denotes the velocity gradient. The scaling laws for low-frequency behavior are highlighted.

https://dx.doi.org/10.1021/acs.macromol.0c02096
Macromolecules 2020, 53, 10955−10963

blocks along three coordinate directions in various systems are shown in Figure S4 (since the **A** and **B** blocks show similar dynamics as the **C** block, only the MSDs of the **C** blocks are given). As shown, in lamellar structures, the motions of **C** blocks along the normal of lamellae (*y*-direction) are dramatically suppressed as compared with the movement along the plane of lamellae (*x*- and *z*-directions). The diffusion coefficients of lamellar structures along the *x*- and *z*-directions are in the same order of magnitude as the **D** system shown in Figure S4a. These observations manifest the fact that the polymer chains in lamellar structures can move along the plane of lamellae, leading to the liquid-like viscoelasticity in vertical shearing.

The viscoelastic properties with the shear direction along the normal of lamellae are shown in Figure 4c. It is worth noting that the general lamellar structures (**L1**, **L2**, and **L3**) exhibit a low-frequency plateau in the storage modulus, which is a characteristic response of cubic phases,[36] while the hierarchical lamellar structures ($\mathbf{L_21}$ and $\mathbf{L_22}$) exhibit a frequency dependency of storage modulus. From what has been discussed (see Figure S4), the alignment of lamellar structures (large-length-scale) imposes restrictions on the movement of polymer beads along the *y*-direction. The immobilization of polymer beads along the shear direction (*y*-direction) leads to the solid-like viscoelasticity and the formation of the elastic plateau in the storage modulus. What is more, the results indicate that the appearance of small-length-scale structures has a marked effect on the viscoelasticity. In principle, the alignment of **A** and **B** blocks along the normal of the lamellar plane (*y*-direction) in the hierarchical structures ($\mathbf{L_21}$ and $\mathbf{L_22}$) would prevent the sliding along the shear direction. However, the sliding of polymers is still possible due to the weaker segregation between **A** and **B** blocks in small-length-scale lamellae (smaller a_{AB} and shorter block). The lack of elastic plateau in the storage modulus for hierarchical structures is ascribed to the ability of the polymer beads to move along the shear direction. Compared with the moduli obtained from three shear directions shown in Figure 4, it is evident that both G' and G'' of lamellae under vertical shear are the smallest, and those under transverse shear are the largest among those under all three shearing ways.

3.3. Relative Magnitudes of the Moduli of Various Structures. In addition to the dependence of moduli on frequency, we further compared the relative magnitude of the moduli of various structures. Figure 5 shows the G' and G'' under parallel shear without any shift. Evidently, there is an enhancement both in the G' and G'' with the formation of large-length-scale structures, especially at low frequency. With the appearance of small-length-scale structures, the G' and G'' further increase over the entire frequency range. The obtained results indicate that the microphase-separated structures have a significant impact on the rheological response. The materials with hierarchical structures exhibit improved viscoelastic properties compared to the general materials with single-periodic nanostructures. This result coincides with our previous finding that the hierarchical lamellae-in-lamellar structures exhibit considerably improved mechanical properties compared to the general lamellar structures.[28]

Under vertical shear, we noted that the G' and G'' of various lamellae are indistinguishable and are close to those of disordered state (see Figure S5). The hierarchical structures do not exhibit enhanced G' and G'' relative to general lamellae and disorder system in vertical shear. However, it is different

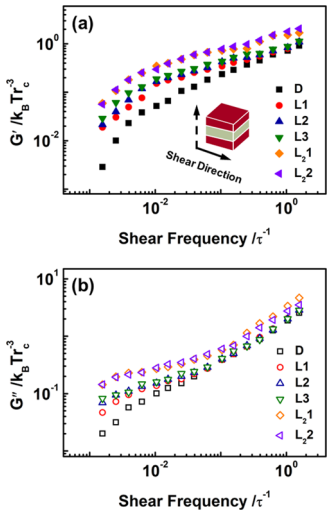

Figure 5. (a) Storage and (b) loss moduli as a function of shear frequency for various structures with parallel shear. Inset in plot (a) is schematic illustration of parallel shear, where the solid arrow represents shear direction, and the dashed arrow denotes the velocity gradient.

for the case under transverse shear (see Figure S6). As shown in Figure S6, both the storage and loss moduli of general lamella increase slightly with increasing the interaction strength between **A** and **B** blocks. The friction applied to the beads has a slight raise upon increasing the **A**/**B** interaction, and this results in the enhancement of dynamic moduli. However, as the morphology transforms from lamella to lamellae-in-lamella, there is an evident decline in the storage modulus. The phase separation interface between **A** and **B** blocks formed under this condition is still weak, and therefore, the polymers in small-length-scale structures can slip along the shear direction, leading to a decrease of G' and vanishing of the elastic plateau. As the interaction between **A** and **B** blocks increases further, the interface in small-length-scale becomes strong, bringing out the recovery of G' (the increase of G' and reappearance of the elastic plateau).

To deepen the understanding of the physical origin underlying the enhanced viscoelasticity of hierarchical structures in parallel shear, we calculated the MSDs of **A**, **B**, and **C** blocks in the *x*-direction (shear direction) for various systems, which is shown in Figure S7. It should be noted that the MSDs of polymer chains in lamellar structures along *x*- and *z*-directions are close due to isotropic characteristics in the lamellar plane. One can see that all the motions of **A**, **B**, and **C** beads exhibit similar tendency and obey diffusion behavior (*i.e.*, the MSDs is proportional to the time) in the long time scales. We can obtain diffusion coefficients by linear fitting of MSD curves. The results for **A**, **B**, and **C** blocks are shown in Figure 6. As can be seen, the diffusion coefficients for **A**, **B**, and **C** blocks are almost the same for each structure. The diffusion coefficients of **B** block, for example, are $2.11 \times 10^{-3}\ r_c^2/\tau$, $1.52 \times 10^{-3}\ r_c^2/\tau$, $1.53 \times 10^{-3}\ r_c^2/\tau$, $1.49 \times 10^{-3}\ r_c^2/\tau$, $1.20 \times 10^{-3}\ r_c^2/\tau$, and $1.32 \times 10^{-3}\ r_c^2/\tau$ in the **D**, **L1**, **L2**, **L3**, $\mathbf{L_21}$, and $\mathbf{L_22}$ systems, respectively. Compared to the **D** system, the diffusion coefficients in the general lamellar systems and hierarchical lamellar systems reduce markedly. Additionally, the diffusion coefficients in hierarchical lamellar systems have lower values relative to general lamellar systems. The value of these diffusion coefficients manifests that the motions of whole

https://dx.doi.org/10.1021/acs.macromol.0c02096
Macromolecules 2020, 53, 10955−10963

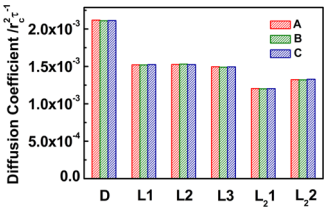

Figure 6. Diffusion coefficients of **A**, **B**, and **C** blocks along the *x*-direction for various structures.

polymer chains slow down with the formation of large-length-scale and small-length-scale structures, which leads to slower stress relaxation and higher dynamic moduli.

3.4. Linear Viscoelasticity of Perpendicular Lamellar Structure. The perpendicular lamellar structure, as previously reported by Bates and Fleury, shows distinct mechanical properties in experiments.[10] In this subsection, we focused on the linear viscoelasticity of perpendicular lamellae-in-lamella. It should be noted that the orientation of small-length-scale structure in the perpendicular lamellae-in-lamellar system has an influence on the viscoelasticity. In our simulations, the adjustment of proper alignment of small-length-scale is difficult, and therefore, we studied the viscoelastic properties of perpendicular lamellar structure with an arbitrary arrangement of small-length-scale lamellae.

Figure 7 shows the frequency sweeps of G' and G'' for the perpendicular lamellae-in-lamellar structure with parallel,

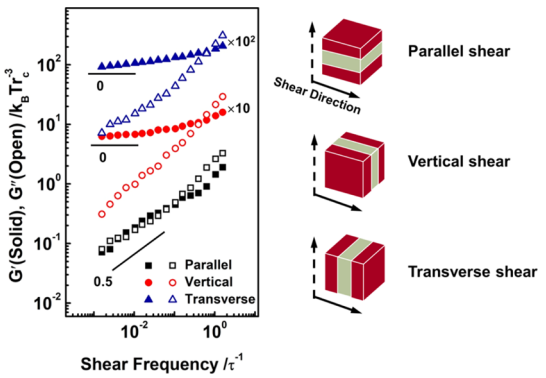

Figure 7. Vertically modulus-shifted master curves for the G' and G'' of perpendicular lamellae-in-lamellar structure with parallel, vertical, and transverse shear. The shift factors are given at the side of each curve. The right shows schematic illustrations of three shearing ways, where the solid arrow represents the shear direction, and the dashed arrow denotes the velocity gradient. The scaling laws for low-frequency behavior are highlighted.

vertical, and transverse shearing. In parallel shear, perpendicular lamellae-in-lamella shows frequency dependences of G' and G'' ($G' \sim G'' \sim \omega^{0.5}$) at low frequency. Two crossovers (ω_c and ω_d) were observed in the curves of G' and G'' plots. The value of ω_c, characterizing the motion of large-length-scales, is close to those in parallel lamellae-in-lamella (**$L_2$1** and **$L_2$2**, see Figure 4a). In addition, the value of ω_d, characterizing the motion of small-length-scales, is close to those in the **L1** system. The rheological responses of perpendicular lamellae-in-lamella in the vertical and transverse shear direction show similar frequency dependence. The solid-like behavior ($G' \sim \omega^0$) appears in these two shear directions. It can be seen that the G' acquired by the parallel shear is an order of magnitude smaller than those obtained by the vertical and transverse shear. Also, the G' obtained by transverse shearing is slightly larger than that obtained by vertical shearing.

The MSDs of **A**, **B**, and **C** blocks along three axial directions were plotted for a deep understanding of the distinct viscoelasticity of the perpendicular hierarchical structures. Figure 8 shows the MSD curve of **B** block along three axes.

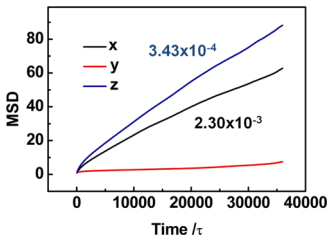

Figure 8. Mean square displacements (MSDs) of **B** blocks along three axes as a function of simulation time in $\mathbf{L}_\perp$ system. The diffusion coefficients along *x* and *z*-directions are highlighted in the plot.

Also, the MSD curves of **A** and **C** blocks are shown in Figure S8. We can see that the **A**, **B**, and **C** blocks show similar diffusive behaviors. The diffusion coefficients of **B** block are also presented in Figure 8. The diffusion coefficients in *x*- and *z*-directions have the values of $2.30 \times 10^{-4}\ r_c^2/\tau$ and $3.43 \times 10^{-4}\ r_c^2/\tau$, respectively. It should be noted that the difference of diffusion coefficients in *x*- and *z*-directions derives from the orientation of small-length-scale structures. Compared to the parallel hierarchical lamellar systems (see Figure 6), the diffusion coefficients in the perpendicular lamellar system along *x*- and *z*-directions are reduced by one order of magnitude, which may result in the formation of the elastic plateau in the storage modulus with the vertical shearing. The reason why the stress cannot be relaxed in the transverse direction is that the large-length-scale structure suppresses the motion of polymer beads, which is the same as the parallel lamellae. Due to the existence of orthogonal two-length-scale structures in the perpendicular lamellae-in-lamella, the whole chain of the polymer cannot move along the shear direction to relax stress, resulting in a low-frequency plateau in the storage modulus by vertical shearing.

This study has shown that there are dramatic differences in the rheological behaviors between the parallel and perpendicular lamellae-in-lamellae with various shear directions. Firstly, in parallel shear, both the parallel and perpendicular hierarchical lamellae exhibit two distinct crossovers. The transition points at a lower frequency (ω_c, corresponding to the longest relaxation time) for these lamellae have similar values, which is ascribed to the large-length-scale relaxation. The appearance of small-length-scale in the perpendicular hierarchical lamella slows down the motion of polymer chains along the plane of the large-length-scale lamella. As a result, the high-frequency transition point (ω_d, corresponding to the relaxation time of small-length-scale) takes place at a lower frequency compared to the parallel hierarchical lamellae. Secondly, in vertical shear, the perpendicular lamella-in-lamellar structure shows distinct viscoelasticity from the parallel lamella-in-lamellar structure. A low-frequency plateau in the storage modulus was found for the perpendicular hierarchical lamella, while the terminal behavior of $G' \sim \omega^2$ and $G'' \sim \omega^1$ was observed in the parallel hierarchical lamellae. The existence of small-length-scale structures in the

https://dx.doi.org/10.1021/acs.macromol.0c02096
Macromolecules 2020, 53, 10955−10963

perpendicular hierarchical lamella suppresses the motions of the polymer chain, leading to the elastic plateau in the vertical shear. Finally, in transverse shear, the perpendicular hierarchical lamellae exhibit an elastic plateau, similar to the behaviors of general lamellae. The weak interface between **A** and **B** blocks exists in the $\mathbf{L_21}$ system due to the weak phase separation in **A** and **B** phases, which results in the frequency-dependence of dynamic modulus in parallel lamella-in-lamellae. In the $\mathbf{L_22}$ system with intense phase separation between **A** and **B** blocks (larger interaction parameter, a_{AB} = 80), the elastic plateau reappears at low frequencies.

3.5. Comparison with Existing Experimental Findings. The present study has shown that the hierarchical structures show distinct viscoelastic properties relative to the disordered structure and general lamellae. We, therefore, compared this observation with existing experimental findings. Bates and Fleury studied the rheological properties of several samples of CECEP hexablock copolymers that can self-assemble into perpendicular lamellae-in-lamellar structures.[10] They demonstrated that the power-law exponents of the G' and G'' plots are 0.5 in the low-frequency region, which is similar to those in general lamellae.[36] Moreover, remarkable improvements of both G' and G'' of these samples were observed upon the formation of small-length-scale structures. In our simulations, the perpendicular lamellae-in-lamella structure exhibits the same rheological behavior of $G' \sim G'' \sim \omega^{0.5}$ in parallel shear, but shows solid-like viscoelasticity in the vertical and transverse shear. We noted that the structures of the experimental samples are macro-disordered and micro-ordered, and therefore, the total rheological behavior is a combination of the rheologies under various shear directions. Our simulation results imply that the parallel shear dominates the rheological behavior of the experimental sample despite the macro-disorder.

We also found that the shear direction imposed on lamellar structures exerts a profound influence on the viscoelastic response of ordered multiblock copolymer melts. Some experimental results in the literature are available to support the simulation results. For instance, Koppi *et al.* studied the linear rheology of oriented lamellae comprised of poly(ethylene-propylene)-poly(ethyl ethylene) diblock copolymers.[40] They found that the storage modulus of lamellae in transverse shear is larger than that in parallel shear, and the storage modulus of lamellae in parallel shear is larger than that in vertical shear. Their observations are consistent with our findings, but there is still some difference. For example, the elastic plateau of storage modulus in transverse shear was not observed in their experiments, which could be ascribed to the lack of bridging conformation in the diblock copolymer and the weaker separation at the interfaces.[41−43]

Riise *et al.* prepared general lamellae formed by the triblock copolymers of styrene and isoprene and found that the lamellae under vertical shear show nearly terminal rheological behavior at low frequencies,[41] which was also observed in our simulations (see Figure 4b). By using large amplitude oscillatory shear to achieve uniaxially oriented cylinders, Ryu *et al.* prepared aligned cylinder samples that adopt hexagonal microstructures with polystyrene cylinders embedded in a polyisoprene matrix.[44] They found that the storage modulus of cylinders sheared parallel to the cylinder axis is less than that sheared perpendicular to the cylinder axis, which is attributed to the sliding of polymer along the axis of the cylinders. These experimental observations agree with our results that the lamellar structures exhibit lower storage and loss moduli in the vertical shear than those in the two other directions, which is related to the motions of polymer chain along the lamellar plane (see Figure 4).

In general, the experimental samples are a larger system and contain many domains with grain boundaries. To compare with the experiment, we built a lamellar structure containing many oriented domains in a larger box by inputting lamellae with different orientations and relaxing them into a metastable structure. Figure S9a shows the structure we acquired. As shown, the artificial structure contains various oriented domains with grain boundaries. Figure S9b shows the storage and loss moduli of the corresponding structure with various shear directions. One can see that there is some difference in storage and loss moduli for lamellae under various shearing directions, which may be ascribed to imperfect isotropic characteristics induced by limited box size. Nonetheless, the moduli at various shearing directions show similar frequency dependency ($G' \sim G'' \sim \omega^{0.5}$). As such, we can deduce that the hierarchical structures with many randomly oriented domains show a frequency dependency of $G' \sim G'' \sim \omega^{0.5}$, which is consistent with the experimental finding.[10]

The simulation is capable of centering the research on a specific influence factor among a series of possibilities, and therefore, we can straightforwardly examine the contribution of hierarchical structures with various shear directions to viscoelasticity. The present work indicates that whether the hierarchical structures can enhance the viscoelastic properties or not depends on the shear direction. Under parallel shear, the viscoelastic properties are improved dramatically as the large-length-scale and/or small-length-scale structures are formed by increasing the interaction parameters. Under vertical shear, however, the general lamellae and parallel lamellae-in-lamella show terminal behaviors at low frequency, and their dynamic moduli are almost identical to those of disordered phases. Under transverse shear, the moduli show a decrease at the onset of phase separation into small-length-scale structures, followed by an increase as the interaction parameters further increase. The work suggests three routes to improve the dynamic moduli: (1) well align the lamellae and impose the transverse shear, (2) increase the interaction between **A** and **B** blocks to generate hierarchical lamellae with strong-segregated small-length-scale lamellae, and (3) design perpendicular hierarchical lamellae to reduce the influence of shear directions.

4. CONCLUSIONS

We employed the nonequilibrium dissipative dynamics simulation to study the viscoelastic properties of heptablock copolymers with various hierarchical lamellar structures in the melts. The viscoelasticity of ordered systems was systematically investigated by imposing three shearing ways, including parallel, vertical, and transverse shearing. It was found that the viscoelasticity is closely associated with the shear direction and packing of lamellar structures. The morphology transformation from lamella to lamellae-in-lamella brings about the significant improvement of moduli in the parallel shear and non-monotonic change of moduli in the transverse shear, but nearly unchanged moduli in the vertical shear. Unlike the frequency-dependent moduli observed for the parallel lamellae-in-lamella, a low-frequency plateau in the storage modulus was found for the perpendicular lamellae-in-lamella in vertical and transverse shear. Moreover, in parallel shear, the parallel

https://dx.doi.org/10.1021/acs.macromol.0c02096
Macromolecules 2020, 53, 10955−10963

lamellae-in-lamella shows enhanced storage and loss moduli compared to the perpendicular lamellae-in-lamella. Our research revealed the physical origin of distinct viscoelasticity of lamellar structures by analyzing the motion of various blocks and could provide useful information for designing hierarchical materials with improved viscoelastic properties.

■ ASSOCIATED CONTENT

Supporting Information

The Supporting Information is available free of charge at https://pubs.acs.org/doi/10.1021/acs.macromol.0c02096.

Full details include DPD, normal coordinates, MSD, comparison of storage and loss moduli between various structures, and MSDs of various blocks (PDF)

■ AUTHOR INFORMATION

Corresponding Authors

Jiaping Lin − *Shanghai Key Laboratory of Advanced Polymeric Materials, Key Laboratory for Ultrafine Materials of Ministry of Education, Frontiers Science Center for Materiobiology and Dynamic Chemistry, School of Materials Science and Engineering, East China University of Science and Technology, Shanghai 200237, China;* orcid.org/0000-0001-9633-4483; Email: jlin@ecust.edu.cn

Liquan Wang − *Shanghai Key Laboratory of Advanced Polymeric Materials, Key Laboratory for Ultrafine Materials of Ministry of Education, Frontiers Science Center for Materiobiology and Dynamic Chemistry, School of Materials Science and Engineering, East China University of Science and Technology, Shanghai 200237, China;* orcid.org/0000-0002-5141-8584; Email: lq_wang@ecust.edu.cn

Authors

Wei Hong − *Shanghai Key Laboratory of Advanced Polymeric Materials, Key Laboratory for Ultrafine Materials of Ministry of Education, Frontiers Science Center for Materiobiology and Dynamic Chemistry, School of Materials Science and Engineering, East China University of Science and Technology, Shanghai 200237, China*

Xiaohui Tian − *Shanghai Key Laboratory of Advanced Polymeric Materials, Key Laboratory for Ultrafine Materials of Ministry of Education, Frontiers Science Center for Materiobiology and Dynamic Chemistry, School of Materials Science and Engineering, East China University of Science and Technology, Shanghai 200237, China*

Complete contact information is available at: https://pubs.acs.org/10.1021/acs.macromol.0c02096

Notes

The authors declare no competing financial interest.

■ ACKNOWLEDGMENTS

This work was supported by the National Natural Science Foundation of China (51833003, 51621002, 21774032, and 21975073).

■ REFERENCES

(1) Fredrickson, G. H.; Bates, F. S. Dynamics of Block Copolymers: Theory and Experiment. *Annu. Rev. Mater. Sci.* **1996**, *26*, 501−550.

(2) Zuo, F.; Alfonzo, C. G.; Bates, F. S. Structure and Mechanical Behavior of Elastomeric Multiblock Terpolymers Containing Glassy, Rubbery, and Semicrystalline Blocks. *Macromolecules* **2011**, *44*, 8143−8153.

(3) Scheirs, J.; Priddy, D. B. *Modern Styrenic Polymers: Polystyrenes and Styrenic Copolymers*; John Wiley & Sons: New York, 2003.

(4) Bates, F. S.; Hillmyer, M. A.; Lodge, T. P.; Bates, C. M.; Delaney, K. T.; Fredrickson, G. H. Multiblock Polymers: Panacea or Pandora's Box? *Science* **2012**, *336*, 434−440.

(5) Yavitt, B. M.; Gai, Y.; Song, D.-P.; Winter, H. H.; Watkins, J. J. High Molecular Mobility and Viscoelasticity of Microphase-Separated Bottlebrush Diblock Copolymer Melts. *Macromolecules* **2017**, *50*, 396−405.

(6) Arun, A.; Dullaert, K.; Gaymans, R. J. The Melt Rheological Behavior of AB, ABA, BAB, and (AB)n Block Copolymers with Monodisperse Aramide Segments. *Polym. Eng. Sci.* **2010**, *50*, 756−761.

(7) Masuda, J.; Takano, A.; Nagata, Y.; Noro, A.; Matsushita, Y. Nanophase-Separated Synchronizing Structure with Parallel Double Periodicity from an Undecablock Terpolymer. *Phys. Rev. Lett.* **2006**, *97*, 098301.

(8) Masuda, J.; Takano, A.; Suzuki, J.; Nagata, Y.; Noro, A.; Hayashida, K.; Matsushita, Y. Composition-Dependent Morphological Transition of Hierarchically-Ordered Structures Formed by Multiblock Terpolymers. *Macromolecules* **2007**, *40*, 4023−4027.

(9) Fleury, G.; Bates, F. S. Perpendicular Lamellae in Parallel Lamellae in a Hierarchical CECEC-P Hexablock Terpolymer. *Macromolecules* **2009**, *42*, 1691−1694.

(10) Fleury, G.; Bates, F. S. Structure and Properties of Hexa- and Undecablock Terpolymers with Hierarchical Molecular Architectures. *Macromolecules* **2009**, *42*, 3598−3610.

(11) Deng, S.; Huang, Y.; Lian, C.; Xu, S.; Liu, H.; Lin, S. Micromechanical Simulation of Molecular Architecture and Orientation Effect on Deformation and Fracture of Multiblock Copolymers. *Polymer* **2014**, *55*, 4776−4785.

(12) Arman, B.; Reddy, A. S.; Arya, G. Viscoelastic Properties and Shock Response of Coarse-Grained Models of Multiblock versus Diblock Copolymers: Insights into Dissipative Properties of Polyurea. *Macromolecules* **2012**, *45*, 3247−3255.

(13) Soto-Figueroa, C.; Rodríguez-Hidalgo, M.-d. -R.; Martínez-Magadán, J.-M. Molecular Simulation of Diblock Copolymers; Morphology and Mechanical Properties. *Polymer* **2005**, *46*, 7485−7493.

(14) Seitz, J. T. The Estimation of Mechanical Properties of Polymers from Molecular Structure. *J. Appl. Polym. Sci.* **1993**, *49*, 1331−1351.

(15) Markov, V.; Kriksin, Y.; Erukhimovich, I.; ten Brinke, G. Perpendicular Lamellar-in-Lamellar and Other Planar Morphologies in A-b-$(B\text{-}b\text{-}A)_2$-b-C and $(B\text{-}b\text{-}A)_2$-b-C Ternary Multiblock Copolymer Melts. *J. Chem. Phys.* **2013**, *139*, 084906.

(16) Klymko, T.; Markov, V.; Subbotin, A.; Brinke, G. t. Lamellar-in-Lamellar Self-Assembled C-b-$(B\text{-}b\text{-}A)_m$-b-B-b-C Multiblock Copolymers: Alexander-de Gennes Approach and Dissipative Particle Dynamics Simulations. *Soft Matter* **2009**, *5*, 98−103.

(17) Zhu, X.; Wang, L.; Lin, J.; Zhang, L. Ordered Nanostructures Self-Assembled from Block Copolymer Tethered Nanoparticles. *ACS Nano* **2010**, *4*, 4979−4988.

(18) Xu, Y.; Li, W.; Qiu, F.; Yang, Y.; Shi, A.-C. Stability of Perpendicular and Parallel Lamellae within Lamellae of Multiblock Terpolymers. *J. Phys. Chem. B* **2010**, *114*, 14875−14883.

(19) Li, W.; Shi, A.-C. Theory of Hierarchical Lamellar Structures from $A(BC)_nBA$ Multiblock Copolymers. *Macromolecules* **2009**, *42*, 811−819.

(20) Liu, H.-H.; Huang, C.-I.; Shi, A.-C. Self-Assemble of Linear ABCBA Pentablock Terpolymers. *Macromolecules* **2015**, *48*, 6214−6223.

(21) Wang, L.; Lin, J.; Zhang, L. Hierarchically Ordered Microstructures Self-Assembled from $A(BC)_n$ Multiblock Copolymers. *Macromolecules* **2010**, *43*, 1602−1609.

(22) Zhang, X.; Wang, L.; Zhang, L.; Lin, J.; Jiang, T. Controllable Hierarchical Microstructures Self-Assembled from Multiblock Copolymers Confined in Thin Films. *Langmuir* **2015**, *31*, 2533−2544.
(23) Hajizadeh, E.; Todd, B. D.; Daivis, P. J. Shear Rheology and Structural Properties of Chemically Identical Dendrimer-Linear Polymer Blends through Molecular Dynamics Simulations. *J. Chem. Phys.* **2014**, *141*, 194905.
(24) Xu, P.; Lin, J.; Wang, L.; Zhang, L. Shear Flow Behaviors of Rod-Coil Diblock Copolymers in Solution: A Nonequilibrium Dissipative Particle Dynamics Simulation. *J. Chem. Phys.* **2017**, *146*, 184903.
(25) Xu, P.; Lin, J.; Zhang, L. Supramolecular Multicompartment Gels Formed by ABC Graft Copolymers: High Toughness And Recovery Properties. *Phys. Chem. Chem. Phys.* **2018**, *20*, 15995−16004.
(26) Sliozberg, Y. R.; Andzelm, J. W.; Brennan, J. K.; Vanlandingham, M. R.; Pryamitsyn, V.; Ganesan, V. Modeling Viscoelastic Properties of Triblock Copolymers: A DPD Simulation Study. *J. Polym. Sci., Part B: Polym. Phys.* **2010**, *48*, 15−25.
(27) Xu, P.; Lin, J.; Zhang, L. Distinct Viscoelasticity of Nanoparticle-Tethering Polymers Revealed by Nonequilibrium Molecular Dynamics Simulations. *J. Phys. Chem. C* **2017**, *121*, 28194−28203.
(28) Zhu, X.; Wang, L.; Lin, J. Distinct Elastic Response to Hierarchical Nanostructures. *Macromolecules* **2011**, *44*, 8314−8323.
(29) Alfonzo, C. G.; Fleury, G.; Chaffin, K. A.; Bates, F. S. Synthesis and Characterization of Elastomeric Heptablock Terpolymers Structured by Crystallization. *Macromolecules* **2010**, *43*, 5295−5305.
(30) Hoogerbrugge, P. J.; Koelman, J. M. V. A. Simulating Microscopic Hydrodynamic Phenomena with Dissipative Particle Dynamics. *Europhys. Lett.* **1992**, *19*, 155−160.
(31) Koelman, J. M. V. A.; Hoogerbrugge, P. J. Dynamic Simulations of Hard-Sphere Suspensions Under Steady Shear. *Europhys. Lett.* **1993**, *21*, 363−368.
(32) Groot, R. D.; Warren, P. B. Dissipative Particle Dynamics: Bridging the Gap between Atomistic and Mesoscopic Simulation. *J. Chem. Phys.* **1997**, *107*, 4423−4435.
(33) Chen, Y.; Li, Z.; Wen, S.; Yang, Q.; Zhang, L.; Zhong, C.; Liu, L. Molecular Simulation Study of Role of Polymer-Particle Interactions in the Strain-Dependent Viscoelasticity of Elastomers (Payne Effect). *J. Chem. Phys.* **2014**, *141*, 104901.
(34) Allen, M. P.; Tildesley, D. *J. Computer Simulation of Liquids*; Oxford University Press: New York, 1989.
(35) LAMMPS Molecular Dynamics Simulator. https://lammps.sandia.gov/(accessed July 22, 2020).
(36) Kossuth, M. B.; Morse, D. C.; Bates, F. S. Viscoelastic Behavior of Cubic Phases in Block Copolymer Melts. *J. Rheol.* **1999**, *43*, 167−196.
(37) Spenley, N. A. Scaling Laws for Polymers in Dissipative Particle Dynamics. *Europhys. Lett.* **2000**, *49*, 534−540.
(38) Doi, M.; Edwards, S. F. *The Theory of Polymer Dynamics*; Oxford University Press: Oxford, U.K., 1986.
(39) Pryamitsyn, V.; Ganesan, V. Origins of Linear Viscoelastic Behavior of Polymer-Nanoparticle Composites. *Macromolecules* **2006**, *39*, 844−856.
(40) Koppi, K. A.; Tirrell, M.; Bates, F. S.; Almdal, K.; Colby, R. H. Lamellae Orientation in Dynamically Sheared Diblock Copolymer Melts. *J. Phys. II* **1992**, *2*, 1941−1959.
(41) Riise, B. L.; Fredrickson, G. H.; Larson, R. G.; Pearson, D. S. Rheology and Shear-Induced Alignment of Lamellar Diblock and Triblock Copolymers. *Macromolecules* **1995**, *28*, 7653−7659.
(42) Mori, Y.; Lim, L. S.; Bates, F. S. Consequences of Molecular Bridging in Lamellae-Forming Triblock/Pentablock Copolymer Blends. *Macromolecules* **2003**, *36*, 9879−9888.
(43) Phatak, A.; Lim, L. S.; Reaves, C. K.; Bates, F. S. Toughness of Glassy-Semicrystalline Multiblock Copolymers. *Macromolecules* **2006**, *39*, 6221−6228.
(44) Ryu, C. Y.; Lee, M. S.; Hajduk, D. A.; Lodge, T. P. Structure and Viscoelasticity of Matched Asymmetric Diblock and Triblock Copolymers in the Cylinder and Sphere Microstructures. *J. Polym. Sci., Part B: Polym. Phys.* **1997**, *35*, 2811−2823.

https://dx.doi.org/10.1021/acs.macromol.0c02096
Macromolecules 2020, 53, 10955−10963